Efficacy of interleukin-13 receptor–targeted liposomal doxorubicin in the intracranial brain tumor model

Achuthamangalam B. Madhankumar,[1] Becky Slagle-Webb,[1] Xinsheng Wang,[1] Qing X. Yang,[2] David A. Antonetti,[3] Patti A. Miller,[2] Jonas M. Sheehan,[1] and James R. Connor[1]

Departments of [1]Neurosurgery, [2]Radiology, and [3]Cellular and Molecular Biology, Penn State Cancer Institute, Pennsylvania State University College of Medicine, Milton S. Hershey Medical Center, Hershey, Pennsylvania

Abstract

Human glioblastoma tumors selectively express receptors for interleukin 13 (IL-13). In a previous study, we showed that liposomes, when conjugated with IL-13, will deliver chemotherapeutics to a subcutaneous glioma tumor model in mice much more effectively than conventional unconjugated liposomes. Based on this observation, we developed an intracranial brain tumor model in nude mice using human U87 glioma cells. Mice receiving weekly i.p. injections of 15 mg/kg of doxorubicin encapsulated in IL-13–conjugated liposomes had a 5-fold reduction in the intracranial tumor volume over 6 weeks and four of seven animals survived >200 days after tumor implantation. In contrast, the animals receiving unconjugated liposomes with the same doxorubicin concentration did not survive beyond 35 days and there was no evidence of tumor size reduction. The presence of liposomes with doxorubicin in the tumor was shown by taking advantage of the selective expression of IL-13 receptors on the tumor cells and the endogenous fluorescence of doxorubicin. There was no increase in the indices of toxicity in animals receiving the doxorubicin-containing liposomes. Finally, a model of the blood-brain barrier was used to show that the nanovesicles do not harm the endothelial cells yet maintain their toxicity to astrocytoma cells. This approach is necessary to show the efficacy of this targeting platform for tumors in which the blood-brain barrier is not compromised and as a potential use of the nanovesicle system as a surveillance mechanism to prevent recurrence. These data show that IL-13 targeted nanovesicles are a viable option for the treatment of brain tumors. [Mol Cancer Ther 2009;8(3):648–54]

Received 4/24/08; revised 12/19/08; accepted 1/8/09; published OnlineFirst 3/10/09.

Grant support: Tara Leah Witmer Memorial Fund Endowment.

The costs of publication of this article were defrayed in part by the payment of page charges. This article must therefore be hereby marked *advertisement* in accordance with 18 U.S.C. Section 1734 solely to indicate this fact.

Requests for reprints: James R. Connor, Department of Neurosurgery (H110), G.M. Leader Family Laboratory, Penn State University, M.S. Hershey Medical Center, 500 University Drive, Hershey, PA 17033-0850. Phone: 717-531-4541; Fax: 717-531-0091. E-mail: jconnor@psu.edu

doi:10.1158/1535-7163.MCT-08-0853

Introduction

Glioblastoma multiforme is an aggressive high-grade brain tumor with poor prognosis. Because of the diffuse nature of the gliomas, surgical resection is difficult. Presently existing chemotherapies are either ineffective in treating the glioma completely or they share toxicity with normal tissues, limiting potentially effective treatment. Targeted therapy is a viable option to overcome the undesirable side effects of the chemotherapeutic agents; if effective targeting moieties can be developed. Our targeted nanovesicle platform takes advantage of the selective expression of interleukin 13 (IL-13) receptors on astrocytoma cells (1–3). We previously reported that IL-13 receptor–targeted chemotherapies delivered through lipid nanovesicles (liposomes) were effective in targeting glioma tumors in a subcutaneous tumor model (4). There are however significant differences between subcutaneous tumor and intracranial tumors, so extrapolation from the subcutaneous model to brain tumors is not straightforward (5). In order to evaluate the targeted nanovesicles for potential clinical application in brain tumors, we did the current study in an intracranial brain tumor model using our IL-13 targeted platform.

IL-13 is an inflammatory cytokine, which mediates its effect through a complex receptor system. The signaling receptor complex for IL-13 consists of IL-13Rα1, which is a relatively low-affinity receptor; and a second receptor, IL-13Rα2, which binds IL-13 with high-affinity (6–9). IL-13Rα2 has no signaling box motifs and because of its nonsignaling function, behaves as a decoy receptor. IL-13Rα2 is a tumor-specific receptor which is overexpressed in glioblastoma multiforme (1–3). The receptor is not only a marker for glioma tumors but also reflects the metastasizing ability of the tumors (10). These observations make IL-13 attractive as a targeting moiety for nanovesicles. The proof of concept for IL-13 targeting in glioblastoma multiforme has been shown in human trials, but these approaches require direct tumor injection (11, 12) and thus are of limited clinical value. In our most recent study, we showed a high level of efficacy for IL-13 targeted nanovesicles in a subcutaneous tumor following i.p. injection (4). Our primary aim in this investigation was to study the efficacy of our nanovesicle platform in an intracranial brain tumor model.

Materials and Methods

Dipalmitoyl phosphatidylcholine, cholesterol, distearoyl-phosphatidylethanolamine polyethyleneglycol 2000, 1,2-distearoyl-*sn*-glycero-3-phosphoethanolamine-*N*-[maleimide(polyethylene glycol)2000] (ammonium salt) were all

purchased from Avanti Polar Lipids. Doxorubicin, methanol, and *t*-butanol were purchased from Sigma Chemicals. Female athymic nude mice were from Jackson Research Laboratories. The stereotactic apparatus which was used for developing intracranial brain tumors was from Stoelting Stereotactic laboratory standard frame. The Human U87 glioma cell line was purchased from American Type Culture Collection.

Preparation of Liposomes

Liposomes were prepared in a similar method as described in our previous publication (1), with slight modifications in the method and composition. Briefly, dipalmitoyl phosphatidylcholine, cholesterol, distearoyl-phosphatidylethanolamine polyethyleneglycol 2000, 1,2-distearoyl-*sn*-glycero-3-phosphoethanolamine-*N*-(maleimide[polyethylene glycol]2000) in a molar ratio of 10:5:0.5:0.25 were dissolved in methanol and *t*-butanol in a ratio of 1:1 (v/v). A thin lipid film was formed in a round-bottomed flask using a rotary evaporator (Buchi). Subsequently, the film was dried under nitrogen and reconstituted in pH 5.5 ammonium sulfate (155 mmol/L). The resulting multilamellar vesicles were extruded 10 times in a nitrogen pressure-operated extruder (Lipex extruder, Northern Lipids, Inc.) at an extrusion pressure of 300 psi using 100 nm and 50 nm membranes. The liposomes were then dialyzed against PBS (pH 7.4) to exchange the buffer outside the liposomes. A solution of 2 mg/mL stock of doxorubicin was then added to the liposomes with constant stirring and incubated at 55°C for 1 h. Doxorubicin was encapsulated in the liposome by following the pH gradient that exists between the interior and exterior wall of the liposomes. The solution was passed through a column and concentrated in a Centriprep YM-30 concentrator (Millipore) to remove unencapsulated doxorubicin. The amount of doxorubicin encapsulated in the liposomes was determined by disrupting the liposomes in a bath type sonicator in 10% solution of Tween 20 and then quantifying the doxorubicin by measuring the absorption at 492 nm.

Conjugation of Liposomes

Human IL-13 protein was expressed in *Escherichia coli* and purified as described in our previous publication (4). IL-13 protein was thiolated using immunothiolane hydrochloride by reacting the protein with immunothiolane hydrochloride with stirring for 1 h in a molar ratio of 1:40 (protein/immunothiolane). The active thiolated protein was passed through a Sephadex G25M column to remove the excess immunothiolane. The thiolated IL-13 was reacted with maleimide containing liposomes and stirred overnight at 4°C. The following day, unconjugated protein was removed either by passing through a column or by concentration using a protein concentrator with a size exclusion of 30,000 (Centriprep YM-30). The amount of protein conjugated to the liposomes was quantified by Bradford protein assay. The assay was done using the Coomasie plus protein assay reagent (Pierce) according to the instructions of the manufacturer.

Particle Size Analysis and Zeta Potential Measurement

The particle size analysis for the IL-13–conjugated (targeted) liposomes loaded with doxorubicin was done with a light-scattering method using an ALV/DLS/SLS-5022F compact goniometer system (ALV) at room temperature. For this analysis, liposomes at a concentration of 0.5 mg/mL in PBS were used. The hydrodynamic radius at an angle of 90 degrees was measured to determine the average particle size of the liposomes.

In vitro Glioma Tumor Spheroids Model

Multicellular tumor spheroids were developed *in vitro* by the liquid overlay method as described earlier (13, 14). Briefly, 24-well plates were coated with 1% Seaplaque agarose gel in a volume of 0.25 mL. Once the gel is solidified, 1×10^5 cells of human U87 glioma cells were plated in each well with complete media. The cells grew at 37°C for 3 days until single uniform intact spheroids are formed in each well. Once the spheroids were formed, the liposome uptake study was done by incubating rhodamine-labeled IL-13–conjugated liposomes with spheroids at 37°C. After 24 h of incubation, the spheroids were observed under a confocal microscope.

Targeted Liposomes and the Blood-Brain Barrier

An *in vitro* blood-brain barrier (BBB) model was used to investigate the BBB transcytotic property of liposomes (15). Briefly, bovine retinal endothelial cells were cultured on transwell filters for 2 days. Once the cells were 90% confluent, they were serum-starved for another 2 days with 103 nmol/L of hydrocortisone, which increases the tight junction protein occludin, after which, the cells are ready for BBB transport studies (16). The transport study was done in serum-free medium, which was added to the apical chamber (500 μL) and the basal chamber (1.5 mL).

For the transport studies, the liposomes were added to the apical chamber along with RITC-labeled dextran, a fluorescent marker. RITC-dextran acts as a control for tight junction integrity because it is not transported across the BBB (15). Therefore, any increase in dextran transport would indicate a disruption in the integrity of the BBB. To determine transport, 100-μL aliquots were collected every hour from the basal chamber, and after 4 h, a 100 μL aliquot was sampled from the apical chamber. Cytotoxicity experiments were done/did with the media collected from the basal chamber. First, 2.5×10^3 cells (U251 glioma cells) per well were plated in a 96-well plate in a total volume of 150 μL. After 24 h, 50 μL of basal media or apical media collected from each time point was added to the cells and incubated for 48 h. At the end of the incubation, the number of proliferating cells was measured by the colorimetric 3-(4,5-dimethylthiazol-2-yl)-5-(3-carboxymethonyphenol)-2-(4-sulfophenyl)-2H-tetrazolium/phenazine methosulfate assay (Promega).

Intracranial Xenograft in Mice

Female athymic nude mice weighing 20 to 30 g were anesthetized by i.p. injection of ketamine-xylazine (75 mg/kg–5 mg/kg body weight). Human U87 MG cells were used for creating the brain tumor xenograft. The head was held in a horizontal position and 1 million cells in a volume of 10 μL were injected into the caudate putamen region using a small animal stereotactic apparatus. The stereotactic coordinates used for the xenografts were $P = 0.5$, $L = 1.7$,

H = 3.8 mm. The glioma cells were injected slowly for 10 min to avoid elevation in the intracranial pressure or upward cell suspension leakage through the track of the needle. T1-weighted magnetic resonance imaging (MRI) contrast was used to determine that a tumor was established.

T1-Weighed MRI Images

T1-weighted MRI contrast was used to visualize the tumor growth using 7T MR imaging system (Bruker, Biospec GmbH) to visualize the tumor. The mice were anesthetized by inhalation of 1% to 2% isoflurane and placed in a position with the brain located at the center of the coil. Intracranial tumor volume was estimated using gadolinium-enhanced T1-weighed multislice axial fast spin echo images. From these images, the size of the tumor was calculated using the region-of-interest tool available on the Paravision software (Bruker Biospec).

Therapeutic Efficacy in Intracranial Tumor Model

An intracranial tumor was generated as described earlier. Once the tumor size reached 5 mm^3, the animals received one of the following: (*a*) untargeted liposomes carrying doxorubicin (n = 8); (*b*) IL-13 conjugated (targeted) liposomes carrying doxorubicin (n = 8); or (*c*) empty liposomes (n = 2). The amount of liposomes that were injected into the mice corresponds to 15 mg/kg body weight of doxorubicin. The injections were done intraperitoneally once a week. The weight of the mice was followed weekly in all of the groups. T1 weighed MRI contrast imaging was done in all the mice in the groups once weekly to monitor tumor growth. We previously showed that empty liposomes have no effect on tumor growth (4); therefore, only two animals were entered into this control group.

The survival experiment was done on a separate group of animals. The tumor was generated as described previously and a T1 weighed MRI imaging was done 2 weeks after implanting the tumor cells to confirm the presence of tumor in this group of mice. The animals then received weekly i.p. injections of either targeted (n = 7) or untargeted (n = 5) liposomes carrying doxorubicin (15 mg/kg body weight). This group did not undergo weekly MRIs because the process of transporting and anesthetizing the mice weekly proved to have a significant negative effect on mouse survival regardless of treatment strategy or even in the absence of tumor. MRI was done at the end of the experiment to confirm the presence or absence of tumor in the mice.

Immunofluorescence of Brain Sections

In one set of experiments, two mice were sacrificed after 3 weeks of injection of liposomes. The brain was dissected rapidly from the cranium and snap-frozen in isopentane and stored at −80°C overnight. After 24 h, the brains were cut into 10-μm-thick sections. The sections were then fixed in 4% paraformaldehyde. The sections containing the tumor were exposed to a primary antibody for IL-13Rα2 (1:200) overnight at 4°C and then washed thrice for 5 min each with 0.1 mol/L of PBS. To visualize the antibody, the sections were treated with Alexafluor conjugated secondary antibody (1:200; green fluorescence) and 4′,6-diamidino-2-phenylindole (1:1,000) to identify the cell nuclei. The sections were visualized under a fluorescent microscope. This approach enables us to take advantage of the endogenous fluorescence of the doxorubicin in the rhodamine wavelength to determine if doxorubicin can be detected in the tumors.

Toxicity Analysis

After the therapeutic evaluation studies, the mice were anesthetized and 300 μL of blood was collected by cardiac puncture. The serum was analyzed for the expression of glutamic oxaloacetic transaminase, serum glutamic pyruvic transaminase, creatine, and blood-urea nitrogen. All the analyses were done by the Department of Comparative Medicine at Penn State University College of Medicine, Hershey, PA by individuals blinded to the experimental conditions.

Results

Particle Size Distribution and Stability

The particle size of the IL-13 conjugated liposomes with doxorubicin was distributed in a narrow range of 50 to 150 nm, with an average size of 100 nm. The polydispersity index of the liposomes was in the range of 0.1 to 0.2. A

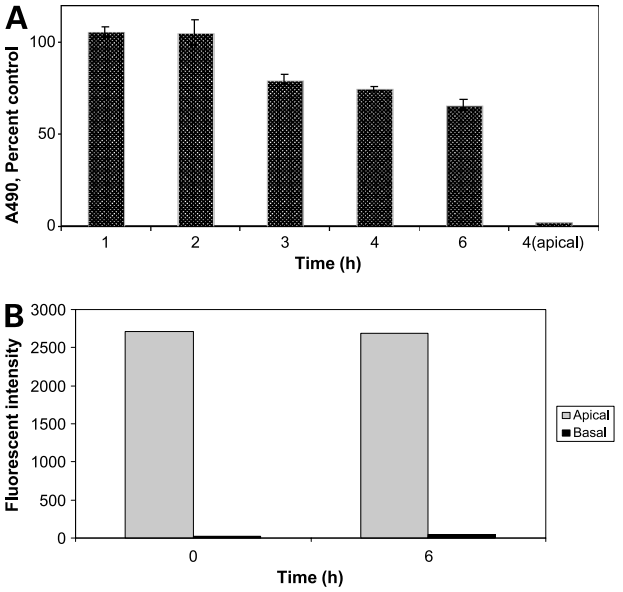

Figure 1. **A,** cytotoxicity experiments done with medium from the BBB transport experiment in the bovine retinal endothelial cell culture model. *Columns,* means of three separate experiments; *bars,* SE. Doxorubicin encapsulated IL-13 conjugated liposomes were added to the apical chamber of the BBB model for 6 h. The medium was collected from the basal chamber at the different time points indicated and placed on U251 glioma cells. Over time, the basal medium becomes more cytotoxic, demonstrating that the targeted liposomes can traverse the endothelial cell layer. There is a high level of cytotoxicity associated with the apical medium after 4 h of treatment with the doxorubicin-encapsulated targeted liposomes, indicating that the endothelial cells were not compromised. **B,** further evidence that the endothelial cells were not compromised was the lack of change in RITC-labeled dextran in the apical or basal medium over the course of the experiments.

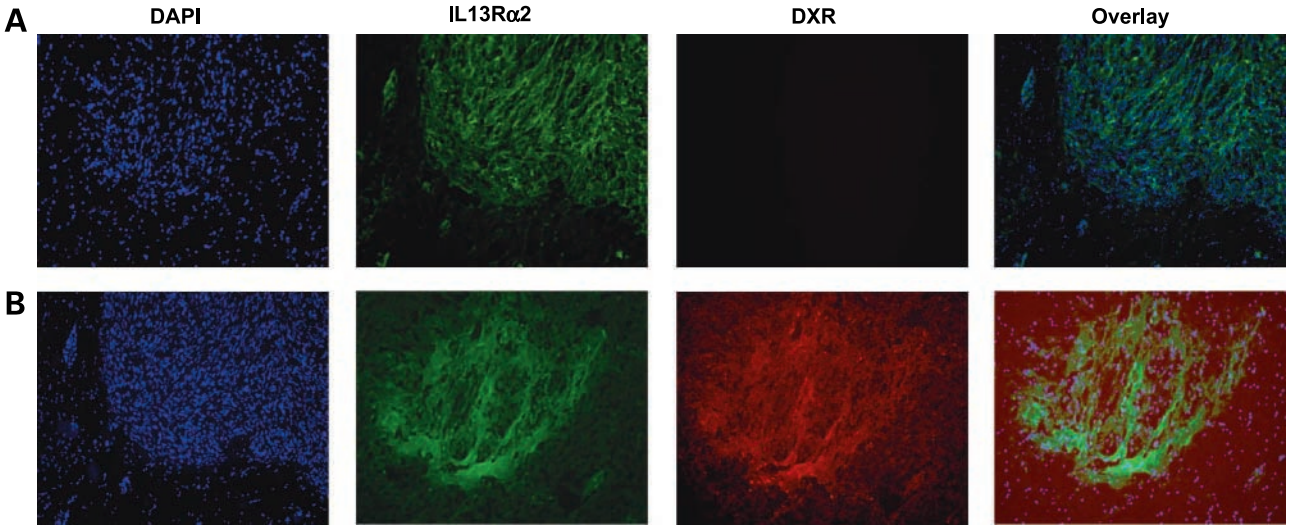

Figure 2. Immunocytochemistry on brain sections containing the intracranial xenografts after administration of untargeted (**A**) or IL-13–targeted (**B**) liposomes containing doxorubicin. The animals were sacrificed 24 h after the administration of a single dose of liposomes containing 15 mg/kg body weight of doxorubicin. *First column,* cells stained with 4′,6-diamidino-2-phenylindole to visualize the cells in the section; *second column,* the distribution of IL-13 receptors in the tumor; *third column,* the distribution of doxorubicin, taking advantage of the endogenous fluorescent activity of this drug; *fourth column,* an overlay of the various images: doxorubicin is confined to the tumor cells in the targeted liposome group and that no drug is detectable in the untargeted group.

representative dynamic light scattering measurement of the formulated liposomes is shown in Supplemental Fig. SF1.[4]

The zeta potential for IL-13 conjugated liposomes was −40 mV (data not shown). The higher negative value results in stable liposomes and a net repulsive force among the liposomes. The doxorubicin encapsulation efficiency of the liposomes was 90%. The liposomes were highly stable with no loss in the particle size or drug leakage for at least 4 weeks at a storage temperature of 4°C. The Bradford assay confirms the presence of protein on the liposomes. The protein concentration of different batches indicated the value to be in the range of 0.04 to 0.15 mg/mL.

In vitro BBB Transport

To investigate if the liposomes could release the cytotoxic agent or themselves damage endothelial cells that form the BBB, we used a cell culture model of the BBB. IL-13 conjugated liposomes encapsulating doxorubicin were placed in the apical chamber of the BBB model. The medium from the basal chamber was collected and placed on cultures of U251 glioma cells. The results show a clear increase in toxicity of the basal medium to the U251 cells the longer the time interval allowed for transport across the BBB model (Fig. 1A). There was no increase in RITC-dextran in the basal medium over the time interval studied, indicating that the integrity of the BBB model was not compromised (Fig. 1B; ref. 17). Cytotoxicity to the astrocytoma cells was calculated as a percentage absorbance at 490 nm after treating the cells with 3-(4,5-dimethylthiazol-2-yl)-5-(3-carboxymethonyphenol)-2-(4-sulfophenyl)-2H-tetrazolium/phenazine methosulfate dye (Fig. 1A).

At the end of the experiment, medium was collected from the apical chamber. This medium was more cytotoxic to the glioma cells than the medium from the basal chamber, indicating that the doxorubicin-encapsulated liposomes did

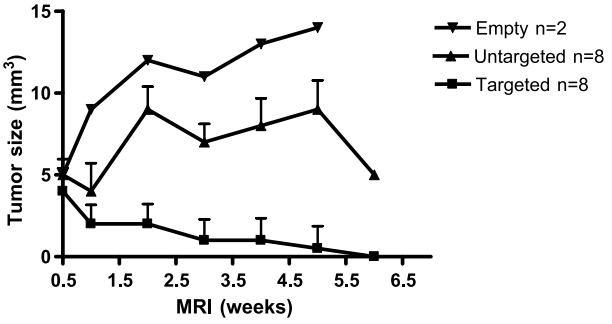

Figure 3. Tumor volume. Animals underwent a MRI every 10 d to follow tumor progression. The mean tumor size is plotted for each time period (*Y axis*). The tumor size was determined from gadolinium-enhanced T1-weighed multislice axial fast spin echo images. The animals received weekly i.p. injections of liposomes. The data show that the tumors in the control animals receiving empty and untargeted nanovesicles grow rapidly and are lethal by 5 wk. The experimental groups of animals received i.p. injections of liposomes that were either conjugated with IL-13 or unconjugated. Both sets of liposomes carried doxorubicin at a concentration of 15 mg/kg body weight. Although the experiment was started with eight animals in each group, at the end of the experiment, only two mice survived in the untargeted group and four mice survived in the targeted group. The tumor size in these surviving animals was similar to the starting volume and did not grow over the course of the study. In contrast, animals receiving targeted liposomes had a significant reduction in tumor size over the course of the study.

[4] Supplementary material for this article is available at Molecular Cancer Therapeutics Online (http://mct.aacrjournals.org/).

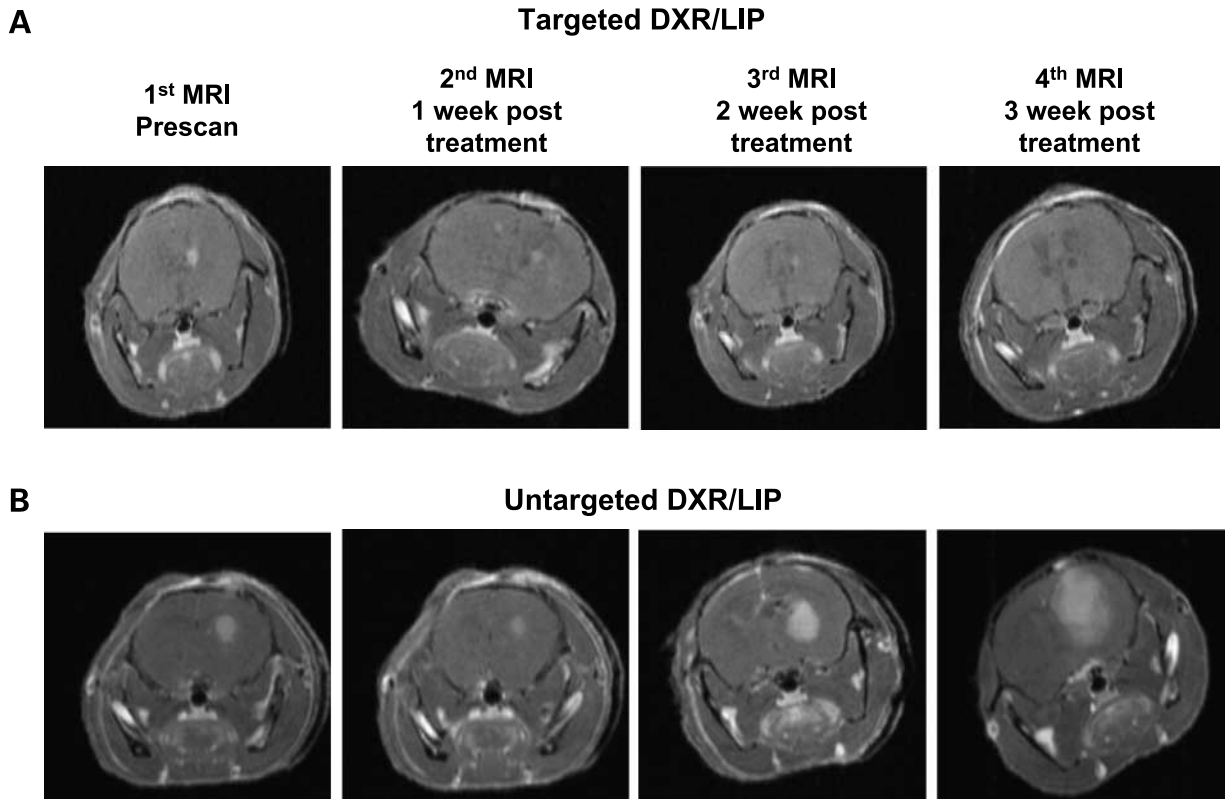

Figure 4. T1 contrast-enhanced brain MRI scan of mice with human U87 astrocytoma cell intracranial xenograft. This is a representative sample of MRIs of the tumors. The images were collected at the times indicated (*top*). The tumor is clearly visible in the pretreatment image for both groups. The tumor decreases in size in (*top*) in animals injected with targeted liposomes carrying doxorubicin. In the animals receiving the untargeted liposomes (*bottom*), after an initial decline in tumor size 1 wk after treatment started (possibly an acute decrease because of the proximity in time to the injection) the tumor continued to enlarge. The outermost concentric shell of highly proliferating neoplastic cells can be seen in mice in the second and third week posttreatment with untargeted liposomes.

not simply diffuse through the BBB layer, and supporting the interpretation that the endothelial cells were not compromised.

Targeting Liposomes to the Intracranial Tumor

To show that IL-13–targeted liposomes accumulate in the tumor, we initially examined a tumor spheroid model in culture. In this model, doxorubicin-containing liposomes could be identified throughout the spheroids, including the core (Supplemental Fig. SF2).[4]

To show that the targeted liposomes with doxorubicin will enter the intracranial tumors in the *in vivo* model, mice were injected i.p. with the targeted and nontargeted liposomes containing doxorubicin. Figure 2A is a representative image that shows doxorubicin (which is endogenously fluorescent) does not accumulate in an intracranial tumor following i.p. injection of nontargeted liposomes, whereas if the liposomes were targeted with IL-13, doxorubicin accumulation is evident (Fig. 2B). The amount of doxorubicin and liposomes and circulation time were the same in each group.

Therapeutic Efficacy of Targeted Liposomal Doxorubicin

To show the therapeutic efficacy of the targeted versus the nontargeted liposomes, mice bearing intracranial tumors of 5 mm^3 (as determined by T1 MRI) received 15 mg/kg body weight of doxorubicin once a week. The size of the tumor decreased from 5 to <1 mm^3 over 6 weeks (Fig. 3) in the group receiving targeted liposomes. Whereas in the group receiving untargeted liposomes with doxorubicin, the tumor volume in the surviving mice (only two of eight) was similar to the starting size (5 mm^3) after 5 weeks. In the mice receiving untargeted nanovesicles that did not carry drug, the tumor volume increased by >100% to 12 mm^3 in 5 weeks. There was a significant decrease in the tumor volume as evidenced by T1 contrast MRI images in the targeted liposome group (Fig. 4).

Survival of the Mice Treated with Targeted Liposomal Doxorubicin

As mentioned, the repeated weekly neuroimaging to monitor the tumor growth negatively affected survival. Therefore, a survival study was conducted in a separate group of mice. The effect of the targeted compared with untargeted nanovesicles on animal survival was determined using a Kaplan-Meier survival graph (Fig. 5). The mean survival of the mice treated with untargeted liposomes was 23 days and no animals survived beyond 35 days. In the animals treated with targeted

liposomes carrying doxorubicin, the mean survival was >100 days and four of the seven mice continues to survive >200 days after tumor formation.

Toxicity Analysis

None of the mice treated with the targeted or untargeted liposomal doxorubicin had abnormal serum chemistry for blood-urea nitrogen or creatine levels, indicating that there was no toxicity to the kidney (Fig. 6). Serum glutamic oxaloacetic transaminase and serum glutamic pyruvic transaminase were comparable to that of the control mice (Fig. 6).

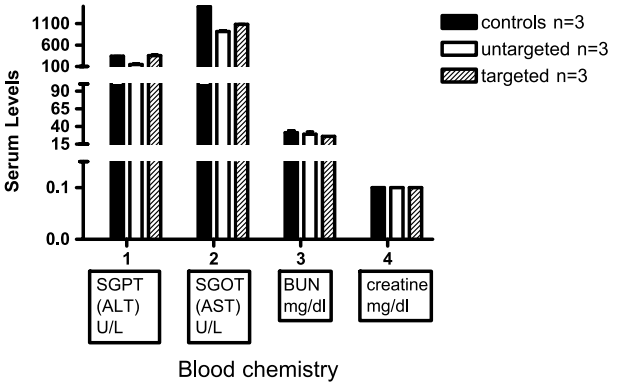

Figure 6. Serum chemistry of mice treated with nontargeted and targeted liposomes. The animals received weekly injections of doxorubicin contained within the liposomes at a concentration of 15 mg/kg body weight for 7 wk. The control group consists of animals with tumors which received injections of PBS. Blood was collected a week after the last injection. Although the mice were treated with what is considered the maximum tolerable dose (in a single injection study) of doxorubicin for 7 wk, these data show that encapsulation of the drug in liposomes was not associated with changes in creatine, blood-urea nitrogen (*BUN*), serum glutamic oxaloacetic transaminase (*SGOT*), or serum glutamic pyruvic transaminase (*SGPT*) values in the serum. *Points,* mean of three animals per group; *bars,* SE.

Discussion

In our previous study, we provided a detailed characterization of our targeted nanovesicle platform and showed proof of concept in a subcutaneous glioma model. That study was the first demonstration of the potential therapeutic efficacy of IL-13–targeted liposomes *in vivo* (4). In the current study, we show the efficacy of an intracranial tumor model; the intended clinical application. We further show that the liposomes do not compromise endothelial cells in a model of the BBB while maintaining their cytotoxicity to astrocytoma cells. The ability to avoid becoming a substrate for P-glycoprotein present in this endothelial cell model (18) is consistent with our previous study that showed packaging of doxorubicin in nanovesicles increased the cellular accumulation of drug in tumor cells when compared with ''free'' drug (4), but extends this finding to show the ability to traverse the BBB. Our data in the BBB model is also in accordance with several other studies which showed that pegylated liposomes can cross the BBB (19, 20).

A major consideration for liposomal delivery across the BBB and accumulation in tumors is size and charge of the liposomes. Liposomes of particle size <100 nm reportedly localize in the tumors, whereas liposomes >100 nm tend to accumulate in the interstitial space (21). Our particle size analysis revealed a narrow distribution and a low polydispersity index (PDI). The low PDI is consistent with our demonstration that the nanovesicles crossed the BBB model and accumulated in the intracranial tumors in both the *in vivo* and cell culture models. The higher negative zeta potential value (−40 mV) in our targeted nanovesicles is associated with a more thermodynamically stable formulation with minimal aggregation, and is consistent with the stability data previously reported (4). The noncationic nature of the liposome formulation is also consistent with the nontoxic behavior of the liposomes *in vitro* and *in vivo* models.

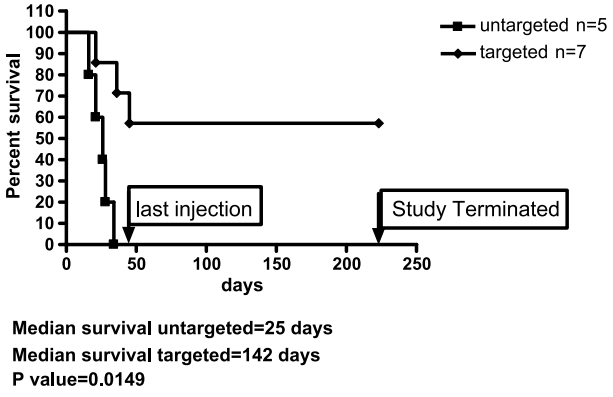

Figure 5. Kaplan-Meier survival graph. Mice received an intracranial xenograft of human U87 astrocytoma cells and were subsequently treated with IL-13 targeted or untargeted liposomes containing doxorubicin at a concentration of 15 mg/kg body weight. The overall survival of the mice receiving targeted liposomes was more than four times higher than in the mice receiving untargeted liposomes. In the group receiving the targeted nanovesicles, four out of seven animals survived for >200 d after their final injection and appeared in good health when sacrificed. For the survival group, the MRI imaging was done only once in the beginning (2 wk after tumor implantation) to confirm tumor formation in the mice.

In addition to the intracranial tumor model, we examined the spheroid tumor model in culture. Tumor spheroid formation is favored under certain conditions like hypoxia, in which there is a limited supply of oxygen and glucose to the core of the spheroids (13). Under such hypoxic conditions, there may be an alteration in the gene profiles due to the elevation in the hypoxia-inducible factor-1α. Moreover, expression of certain mismatch genes due to cell-cell interaction under hypoxic condition may result in chemoresistance. Even in the three-dimensional spheroidal model we used, doxorubicin in the liposomes was found throughout the tumor, indicating that the liposomes can diffuse to the core of the tumor without traversing a blood vessel. Both the *in vivo* and *in vitro* tumor data are consistent with the significant reduction in the rate of tumor growth in the animal groups injected with IL-13 conjugated liposomes carrying doxorubicin.

There is a striking and significant improvement in the mean survival of the mice treated with targeted liposomes

compared with the untargeted liposomes. Comparison of our targeted nanovesicle platform to published data for IL-13 fusion proteins that were directly injected into the intracranial tumor indicates that the targeted nanovesicle approach increases survival by at least 2.5 times (22). Indeed, the targeted nanovesicle approach is even more impressive because the untreated control group in the IL-13 fusion protein study survived 55 days after the tumor implant, whereas the animals in our control group all expired by 35 days, suggesting that the tumors in our study were more aggressive than in the intratumoral injection study (22).

The amount of doxorubicin delivered via the nanovesicles was 15 mg/kg body weight of the mice, which is much higher than the maximal tolerated dose reported in the literature for mice (23). The potential for toxicity was examined directly using serum chemistry. Blood-urea nitrogen and creatine in the serum are indices of renal toxicity, and these measures were not different from controls (no tumors or liposome injections; Fig. 6). The values for serum glutamic oxaloacetic transaminase and serum glutamic pyruvic transaminase, which are the representative measures of liver toxicity, were also not different for the animals receiving the liposomal injections compared with control. These data indicate no toxicity to systemic organs, consistent with the long-term animal survival, despite the relatively high concentrations of doxorubicin that were delivered. The lack of extratumoral toxicity coupled with the survival data provide compelling evidence for the efficacy of liposomal encapsulation of a chemotoxin and targeted delivery.

Disclosure of Potential Conflicts of Interest

No potential conflicts of interest were disclosed.

Acknowledgments

We acknowledge the Pennsylvania State University College of Medicine for the use of their confocal microscopy core facility and the Department of Comparative Medicine for their assistance with the toxicity assays.

References

1. Kawakami M, Leland P, Kawakami K, Puri RK. Mutation and functional analysis of IL-13 receptors in human malignant glioma cells. Oncol Res 2001;12:459 – 67.

2. Husain SR, Puri RK. Interleukin-13 receptor-directed cytotoxin for malignant glioma therapy: from bench to bedside. J Neurooncol 2003;65: 37 – 48.

3. Debinski W, Slagle B, Gibo DM, Powers SK, Gillespie GY. Expression of a restrictive receptor for interleukin 13 is associated with glial transformation. J Neurooncol 2000;48:103 – 11.

4. Madhankumar AB, Slagle-Webb B, Mintz A, Sheehan JM, Connor JR. Interleukin-13 receptor-targeted nanovesicles are a potential therapy for glioblastoma multiforme. Mol Cancer Ther 2006;5:3162 – 9.

5. Blouw B, Song H, Tihan T, et al. The hypoxic response of tumors is dependent on their microenvironment. Cancer Cell 2003;4:133 – 46.

6. Aman MJ, Tayebi N, Obiri NI, Puri RK, Modi WS, Leonard WJ. cDNA cloning and characterization of the human interleukin 13 receptor α chain. J Biol Chem 1996;271:29265 – 70.

7. Caput D, Laurent P, Kaghad M, et al. Cloning and characterization of a specific interleukin (IL)-13 binding protein structurally related to the IL-5 receptor α chain. J Biol Chem 1996;271:16921 – 6.

8. Hilton DJ, Zhang JG, Metcalf D, Alexander WS, Nicola NA, Willson TA. Cloning and characterization of a binding subunit of the interleukin 13 receptor that is also a component of the interleukin 4 receptor. Proc Natl Acad Sci U S A 1996;93:497 – 501.

9. Zhang JG, Hilton DJ, Willson TA, et al. Identification, purification, and characterization of a soluble interleukin (IL)-13-binding protein. Evidence that it is distinct from the cloned IL-13 receptor and IL-4 receptor α-chains. J Biol Chem 1997;272:9474 – 80.

10. Gupta GP, Minn AJ, Kang Y, et al. Identifying site-specific metastasis genes and functions. Cold Spring Harb Symp Quant Biol 2005;70: 149 – 58.

11. Kawakami K, Kioi M, Liu Q, Kawakami M, Puri RK. Evidence that IL-13R α2 chain in human glioma cells is responsible for the antitumor activity mediated by receptor-directed cytotoxin therapy. J Immunother 2005;28:193 – 202.

12. Kawakami K, Terabe M, Kioi M, Berzofsky JA, Puri RK. Intratumoral therapy with IL-13-PE38 results in effective CTL-mediated suppression of IL-13Rα2-expressing contralateral tumors. Clin Cancer Res 2006;12: 4678 – 86.

13. Kobayashi H, Man S, Graham CH, Kapitain SJ, Teicher BA, Kerbel RS. Acquired multicellular-mediated resistance to alkylating agents in cancer. Proc Natl Acad Sci U S A 1993;90:3294 – 8.

14. Francia G, Man S, Teicher B, Grasso L, Kerbel RS. Gene expression analysis of tumor spheroids reveals a role for suppressed DNA mismatch repair in multicellular resistance to alkylating agents. Mol Cell Biol 2004; 24:6837 – 49.

15. Burdo JR, Antonetti DA, Wolpert EB, Connor JR. Mechanisms and regulation of transferrin and iron transport in a model blood-brain barrier system. Neuroscience 2003;121:883 – 90.

16. Antonetti DA, Wolpert EB, DeMaio L, Harhaj NS, Scaduto RC, Jr. Hydrocortisone decreases retinal endothelial cell water and solute flux coincident with increased content and decreased phosphorylation of occludin. J Neurochem 2002;80:667 – 77.

17. Olsson Y, Svensjo E, Arfors KE, Hultstrom D. Fluorescein labelled dextrans as tracers for vascular permeability studies in the nervous system. Acta Neuropathol 1975;33:45 – 50.

18. Ohnishi T, Tamai I, Sakanaka K, et al. *In vivo* and *in vitro* evidence for ATP-dependency of P-glycoprotein-mediated efflux of doxorubicin at the blood-brain barrier. Biochem Pharmacol 1995;49:1541 – 4.

19. Huwyler J, Wu D, Pardridge WM. Brain drug delivery of small molecules using immunoliposomes. Proc Natl Acad Sci U S A 1996;93: 14164 – 9.

20. Shi N, Boado RJ, Pardridge WM. Receptor-mediated gene targeting to tissues *in vivo* following intravenous administration of pegylated immunoliposomes. Pharm Res 2001;18:1091 – 5.

21. Nagayasu A, Uchiyama K, Kiwada H. The size of liposomes: a factor which affects their targeting efficiency to tumors and therapeutic activity of liposomal antitumor drugs. Adv Drug Deliv Rev 1999;40:75 – 87.

22. Rustamzadeh E, Hall WA, Todhunter DA, et al. Intracranial therapy of glioblastoma with the fusion protein DTIL-13 in immunodeficient mice. Int J Cancer 2006;118:2594 – 601.

23. Vanhoefer U, Cao S, Harstrick A, Seeber S, Rustum YM. Comparative antitumor efficacy of docetaxel and paclitaxel in nude mice bearing human tumor xenografts that overexpress the multidrug resistance protein (MRP). Ann Oncol 1997;8:1221 – 8.